

1 **Historical reconstruction of Ocean Acidification in the Australian region**

2

3 Andrew Lenton<sup>1</sup>

4 Bronte Tilbrook<sup>1,2</sup>

5 Richard J. Matear<sup>1</sup>

6 Tristan P. Sasse<sup>3</sup>

7 Yukihiro Nojiri<sup>4</sup>

8

9 <sup>1</sup>CSIRO Oceans and Atmosphere National Research Flagship, Hobart, Australia

10 <sup>2</sup>Antarctic Climate and Ecosystems Co-operative Research Centre, Hobart, Australia

11 <sup>3</sup>Climate Change Research Centre, Kensington Campus, University of New South  
12 Wales, Sydney, Australia

13 <sup>4</sup>National Institute for Environmental Studies, Tsukuba, Japan

14

15 **1. Abstract**

16 The ocean has become more acidic over the last 200 years in response increasing  
17 atmospheric carbon dioxide (CO<sub>2</sub>) levels. Documenting how the ocean has changed is  
18 critical for assessing how these changes impact marine ecosystems, and for the  
19 management of marine resources. Here we use present day ocean carbon  
20 observations, from shelf and offshore waters around Australia, combined with neural  
21 network mapping of CO<sub>2</sub>, sea surface temperature and salinity to estimate the current  
22 seasonal and regional distributions of carbonate chemistry (pH and aragonite  
23 saturation state). The observed changes in atmospheric CO<sub>2</sub> and SST and  
24 climatological salinity are then used reconstruct pH and aragonite saturation state  
25 changes over the last 140 years (1870–2013). The comparison with data collected at  
26 Integrated Marine Observing System National Reference Station sites located on the  
27 shelf around Australia shows both the mean state, and seasonality in the present day is  
28 well represented by our reconstruction, with the exception of sites such as the Great  
29 Barrier Reef. Our reconstruction predicts that since 1870 an average decrease in  
30 aragonite saturation state of 0.48 and of 0.09 in pH has occurred in response to  
31 increasing oceanic uptake of atmospheric CO<sub>2</sub>. Large seasonal variability in pH and  
32 aragonite saturation state occur in Southwestern Australia driven by ocean dynamics  
33 (mixing) and in the Tasman Sea by seasonal warming (in the case of aragonite

34 saturation state). The seasonal and historical changes in aragonite saturation state and  
35 pH have different spatial patterns and suggest that the biological responses to ocean  
36 acidification are likely to be non-uniform depending on the relative sensitivity of  
37 organisms to shifts in pH and saturation state. This new historical reconstruction  
38 provides an important link to biological observations that will help to elucidate the  
39 consequences of ocean acidification.

40

## 41 **2. Introduction**

42 The ocean plays a key role in reducing the rate of global climate change, absorbing  
43 approximately 30% of the anthropogenic CO<sub>2</sub> emitted over the last 200 years (Ciais et  
44 al., 2013), and more than 25% of current CO<sub>2</sub> emissions (Le Quéré, 2015). The CO<sub>2</sub>  
45 taken up by the ocean reacts in seawater, leading to decreases in pH and dissolved  
46 carbonate ion concentrations (CO<sub>3</sub><sup>2-</sup>), these changes being collectively referred to as  
47 ocean acidification. Over the past 200 years, it is estimated that there has been a 0.1  
48 unit reduction in the ocean's surface pH, or 26% increase in the concentration of  
49 hydrogen ion concentrations in seawater (Doney et al., 2009).

50

51 Current projections suggest that the increase in hydrogen ion concentration is likely to  
52 be greater than 100% (than the preindustrial period) by the end of the century under  
53 high emissions trajectories e.g. Matear and Lenton (2014). Furthermore these changes  
54 will persist for many millennia e.g. Frolicher and Joos (2010). Ocean acidification is  
55 likely to impact the entire marine ecosystem - from microbial communities to top  
56 predators. Factors that can be impacted include reproductive health, organism growth  
57 and physiology, species composition and distributions, food web structure and  
58 nutrient availability (Aze et al., 2014; Doney et al., 2012; Dore et al., 2009; Fabry et  
59 al., 2008; Iglesias-Rodriguez et al., 2008; Munday et al., 2010; Munday et al., 2009).

60

61 Aragonite is a metastable form of calcium carbonate that is produced by major  
62 calcifiers in coral reef ecosystems, including reef building corals, and is the  
63 predominant biogenic carbonate mineral in warm and shallow waters of the tropics  
64 (Stanley and Hardie, 1998). The aragonite saturation state of seawater has been used  
65 as a proxy for estimating net calcification rates for corals e.g. Langdon (2005).

66 Projections suggest that by as early as 2050 growth rates of reef building coral may

67 slow to such levels that coral reefs may start to dissolve (Silverman et al., 2009). The  
68 impact of acidification combined with other stressors, such as ocean warming, has  
69 implications for the health, longer-term sustainability and biodiversity of reef  
70 ecosystems (Doney et al., 2012; Dore et al., 2009).

71

72 The impact of these changes on the marine environment is fundamental for the  
73 management of future marine resources, for nations like Australia with its extensive  
74 coastline and regions of international significance such as the Great Barrier Reef. An  
75 historical record of the changes that have occurred since the preindustrial period  
76 allows us to (i) correctly attribute observed responses over the historical period; (ii)  
77 assess how well climate models represent spatial patterns of ocean acidification for  
78 the period that overlaps observations (e.g. IPCC AR5); (iii) quantify the magnitude of  
79 seasonal variability, and identify the drivers of this variability; and (iv) provide  
80 important boundary conditions for high resolution regional models.

81

82 Despite the potential impacts of ocean acidification for the Australian region, the  
83 number of carbonate chemistry measurements remains sparse. The few datasets  
84 collected only characterise variability and the mean state in specific environments e.g.  
85 (Shaw et al., 2012; Albright et al., 2013) or attempt to synthesize these into regional  
86 or habitat-based studies e.g. Gagliano et al. (2010). The only seasonally-resolved  
87 observational dataset available to characterize the mean state around Australia in the  
88 present day is Takahashi et al. (2014), but this data has coarse resolution and only  
89 focuses on the open ocean areas. Studies that have reconstructed the longer-term  
90 variability of ocean acidification from coral proxies have been of regional scale, and  
91 are temporally coarse e.g. Pelejero et al. (2005) and Calvo et al. (2007).

92

93 The goals of our study are: (i) reconstruct the observed variability and mean state in  
94 pH and aragonite saturation state in the present day around Australia at high spatial  
95 resolution and (ii) reconstruct the changes that have occurred in the Australian region  
96 over the last 140 years (1870-2013). To this end, we first develop a new salinity-  
97 alkalinity relationship for Australian waters based on observations collected around  
98 Australia over the last two decades. We then assess our reconstructed pH and  
99 aragonite saturation state fields with data collected around Australia at the Integrated

100 Marine Observing System National Reference Stations (IMOS-NRS; Lynch et al.,  
101 2014). Finally, we present the reconstructed aragonite saturation state and pH in the  
102 Australian region and discuss the seasonal and long-term changes in these fields. The  
103 reconstructed fields as well as the calcite saturation state, dissolved inorganic carbon  
104 dioxide (DIC), total alkalinity (TALK), sea surface temperature and salinity are all  
105 available online at <http://imos.aodn.org.au>.

106  
107

### 108 **3. Methods**

109 In this study we focus on the Australian region (Figure 1) delineated nominally by the  
110 Subtropical Front (45° S) in the south and the equator (0°) in the north, and between  
111 95°E and 170° E. This region encompasses part of the eastern Indian Ocean and  
112 Indonesian Seas and a large part of the Tasman and Coral Seas. The seasonal cycle of  
113 physical, chemical, and biological properties of the surface ocean mixed layer in this  
114 region are described in Condie and Dunn (2006), and will not be described further in  
115 this paper. The characterization of the carbon system requires two of six potential  
116 carbon parameters (i.e. pH, total dissolved inorganic carbon, total alkalinity, partial  
117 pressure of carbon dioxide  $p\text{CO}_2$ , bicarbonate, carbonate), from which all the  
118 parameters of the ocean carbon system can be calculated. We first use  $p\text{CO}_2$  and total  
119 alkalinity to reconstruct the changes in ocean acidification.

120

121 Oceanic values of  $p\text{CO}_2$  were taken from an updated version of Sasse et al. (2013)  
122 that used a self-organizing multiple linear output (SOMLO) approach to predict  $p\text{CO}_2$   
123 values around Australia on a 1° x 1° degree grid each month for the nominal year of  
124 2000. The SOMLO approach utilizes a global network of bottle-derived  $p\text{CO}_2$  and  
125 corresponding standard hydrographic parameters (SHP; temperature, salinity,  
126 dissolved oxygen and phosphate; N=17753), collected from more than 263 cruises  
127 and the HOTS and BATS time series sites, for more information on the individual  
128 cruise data please see Table A1 in Sasse et al (2013). This data was first clustered into  
129 49 neurons (or bins) based on similarities and homogeneity. Principle component  
130 regressions were then derived between  $p\text{CO}_2$  and the SHP using data within each  
131 neuron. This can be thought of as a local-scale optimization, which follows the  
132 nonlinear clustering routine. To then predict  $p\text{CO}_2$  values for any set of SHP, a

133 similarity measure is first used to establish which neuron best represents the SHP  
134 measurements, once established, pCO<sub>2</sub> values are predicted using the regression  
135 parameters of that neuron. Independent testing by Sasse et al. (2013) reveals the  
136 SOMLO approach predicts open-ocean pCO<sub>2</sub> values with a global uncertainty of 22.5  
137 µatm (RMSE), which decreases to 16.3 µatm (RMSE; N=859) within the Australia  
138 region. Monthly pCO<sub>2</sub> climatologies presented in Sasse et al. (2013) were derived  
139 using the World Ocean Atlas (WOA) 2009 product (Antonov et al., 2010; Garcia et  
140 al., 2010a; Garcia et al., 2010b; Locarnini et al., 2010), which we update here via the  
141 WOA 2013 product (Garcia et al., 2014a, b; Locarnini et al., 2013; Zweng et al.,  
142 2013). We note that these pCO<sub>2</sub> values provide significantly higher spatial data  
143 coverage than the global climatology of Takahashi et al. (2009).

144

145 To extend the oceanic pCO<sub>2</sub> values into the past and the future, the value of  $\Delta$  pCO<sub>2</sub>  
146 (pCO<sub>2,air</sub> - pCO<sub>2,sea</sub>) was first calculated using the oceanic pCO<sub>2</sub> values of Sasse et al.  
147 (2013) for the year 2000. This  $\Delta$  pCO<sub>2</sub> value was then transformed into a time series  
148 of oceanic pCO<sub>2</sub> between 1870 to 2013, by adding this to the observed atmospheric  
149 CO<sub>2</sub> value over this period using the atmospheric history constructed by Le Quéré et  
150 al (2015).

151 As only limited measurements of total alkalinity (TALK) exist in the Australian  
152 region, we develop and use the relationship between TALK and salinity to estimate  
153 TALK in the Australian region. While many studies have quantified this relationship  
154 globally e.g. Takahashi et al. (2014) and Lee et al. (2006) and regionally e.g.  
155 Kuchinke et al. (2014), to date no specific relationship has been developed for the  
156 entire Australian region.

157 To develop this relationship 2772 concomitant measurements of salinity and alkalinity  
158 collected in the Australian region over the last two decades were used. (Table 1;  
159 Figure 1). From this data we determined our alkalinity-salinity relationship to be:

160

$$161 \quad \text{TALK } (\mu\text{mol/kg}) = (2270.0 \pm 0.1) + (64.0 \pm 0.3) * (\text{SAL} - 35.) \quad (1)$$

162

163 This relationship is based on a type 2 linear regression, accounting for uncertainty in  
164 both the salinity and TALK measurements of 0.05 and 3 µmol/kg respectively. This

165 new relationship was applied to the climatology of salinity ( $0.5^\circ \times 0.5^\circ/\text{daily}$ ) taken  
166 from the CSIRO Atlas of Regional Seas 2012 (CARS; Ridgway et al., 2002) as no  
167 long-term high spatial and temporal resolution observations of ocean surface salinity  
168 at present exist around Australia (nor globally). Nevertheless, based on sparse  
169 measurements Durack and Wijffels (2010) suggested that there has been an  
170 amplification of the global hydrological cycle that has resulted in surface salinity  
171 changes over the last 50 years. Their estimated changes around Australia are not  
172 uniform and are typically less than  $\pm 0.1$ , which introduces only a  $6.4 \mu\text{mol/kg}$  change  
173 in TALK for the 50-year period. The influence of the changes on the carbonate  
174 chemistry (pH and aragonite saturation state changes of about 0.001 and 0.02  
175 respectively), are small compared to the changes predicted from increasing  
176 atmospheric  $\text{CO}_2$  thereby allowing us to assume that the CARS salinity used has not  
177 changed in our calculations.

178

179 Sea surface temperature (SST) measurements from 1870 to the present day were  
180 obtained from the HadISST v1.1 dataset ( $1^\circ \times 1^\circ$ ; Rayner et al., 2003). Higher  
181 resolution datasets do exist, e.g. NOAA OI V2 ( $0.25^\circ \times 0.25^\circ$ ; Reynolds et al., 2007),  
182 but none have estimates beyond the last 3 decades, and we chose the  $1^\circ \times 1^\circ$  product to  
183 extend our reconstruction back to the pre-industrial period.

184 We first calculated DIC from TALK, SST and  $\text{pCO}_2$  in the period 1870-2013, using  
185 the method following Lenton et al. (2012) that used the dissociation constants of  
186 Mehrbach et al. (1973) refitted by Dickson and Millero (1987). Our implementation  
187 of carbonate chemistry is derived from the OCMIP3 framework (O. Aumont, C. Le  
188 Quéré, and J. C. Orr, NOCES Project Interannual HOWTO, 2004, available at  
189 <http://www.ipsl.jussieu.fr/OCMIP/>).

190

191 This approach calculates the magnitude of the seasonal cycle of DIC, rather than  
192  $\text{pCO}_2$ . The  $\text{pCO}_2$  seasonality changes over time in response to changes in the Revelle  
193 factor and will influence the air-sea gradient in  $\text{pCO}_2$ , which drives net flux across the  
194 air-sea boundary e.g. Hauck and Völker (2015). To correct for this, we first calculated  
195 the (detrended) seasonal anomaly of DIC in the period 1995-2006. We then added this  
196 seasonal cycle of DIC to the (deseasonalised) long-term DIC record (1870-2013).

197 This allows us to reconstruct the historical DIC fields, and the changes in the

198 magnitude of the oceanic pCO<sub>2</sub> in response to the Revelle Factor to be accounted for.

199 We then added this seasonal cycle to the deseasonalised long-term DIC record (1870-  
200 2013) to reconstruct the DIC fields, thereby allowing pCO<sub>2</sub> to change. The  
201 reconstructed DIC fields were then used in conjunction with our derived TALK fields  
202 to calculate changes in ocean acidification in the period 1870-2013. As the resolution  
203 of SST and pCO<sub>2</sub> fields are nominally 1°x1° monthly fields, all values were calculated  
204 on a 1°x1° grid at in-situ temperatures. The values of pH were calculated using the  
205 total scale following recommendations of Riebesell et al. (2010) while aragonite and  
206 calcite saturation states were calculated following Mucci (1983). To assess the  
207 uncertainty in the reconstructed ocean acidification values, we compared these with  
208 the values calculated from individual cruises, this allowed us to estimate the  
209 uncertainty (RSME) to be 0.02 and 0.1 in pH and aragonite saturation state  
210 respectively.

## 211 **4. Results and Discussion**

### 212 **4.1 Assessment of the mean state and seasonal variability at coastal NRS sites**

213 The ability of our reconstruction to predict the mean state and seasonality of ocean  
214 acidification around Australia was evaluated by comparing our calculated aragonite  
215 saturation state and SST data with carbonate chemistry and SST measurements made  
216 over the last few years from seven of the eight Australian IMOS-NRS sites (Figure 2;  
217 <https://imos.aodn.org.au>). The Darwin NRS site was not used in the comparison due  
218 to the small number of measurements at this site. To assess how well the observed  
219 response at the NRS sites were captured, we calculated both the correlation  
220 coefficient (*R*) and the bias (or bias function) shown in Table 2.

221 The observed responses from the NRS sites compared with HadiSST are shown in  
222 Figure 3. There is a good correlation in SST at all sites ( $r > 0.84$ , Table 2) providing  
223 confidence that HadiSST represents the character of the seasonal variability. However  
224 while HadiSST captures the SST variability, there were some biases in the mean SST  
225 value (Table 2). These biases, e.g. Rottneest Island, likely reflect local process in the  
226 coastal environment at the NRS e.g. Lima and Wethey (2012) that are poorly captured  
227 by the much larger spatial scale of the HadiSST product.

228 The reconstructed aragonite saturation state ( $\Omega_{AR}$ ) shows good agreement with values  
229 calculated from observations (Figure 4). The implication is that the salinity - total  
230 alkalinity relationship and calculated  $pCO_2$  fields, which are derived mostly from  
231 offshore data, are valid for most of the IMOS-NRS sites, which tend to be located on  
232 the outer shelf. Exceptions are the Ningaloo and Yongala sites, where our  
233 reconstruction overestimates the observed values of aragonite saturation state while  
234 SST agrees well with HadiSST (Table 2). The total alkalinity - salinity relationship  
235 may not hold at these two sites due to the influence of net calcification on nearby  
236 coral reef systems and possibly sediment-water exchange that could alter the total  
237 alkalinity e.g. Shaw et al. (2012).

238 Apart from the offsets at the Yongala and Ningaloo sites, the reconstructed aragonite  
239 saturation state does recreate the range determined at most locations (e.g. Maria  
240 Island, Port Hacking, Rottneest, and North Stradbroke Island). Limited sampling at  
241 Kangaroo Island, Esperance and Ningaloo sites prevented direct comparisons of the  
242 seasonal variability, although the reconstructed variability appears plausible based on  
243 available measurements.

244 Overall the ability of our reconstruction to capture the mean state and variability of  
245 ocean acidification at the IMOS-NRS sites, gives us confidence in the reconstruction  
246 of ocean acidification in the shelf and offshore waters around Australia, and to extend  
247 our reconstruction back in time.

248

#### 249 **4.2 Annual mean state**

250 The mean state of aragonite saturation state around Australia for the period 2000-2009  
251 is shown in Figure 5. The mean state shows a strong latitudinal gradient in aragonite  
252 saturation increasing from values of 1.8 in the southern part of the domain to values  
253 greater than 3.9 across Northern Australia and into the Coral Sea. The Coral Sea and  
254 Western Pacific form part of the coral triangle, a globally significant region in terms  
255 of coral and marine diversity (Bell et al., 2011). We see that our reconstructed values  
256 in the Coral Sea and into the Western Pacific are also consistent with the  
257 observational values of 3.9 calculated by Kuchinke et al. (2014) in this region. This  
258 value is well above 3.5, considered to be a key threshold at which corals move from



259 healthy to marginal conditions (Guinotte et al., 2003).

260 Ricke et al. (2013), using results from an ensemble of CMIP5 simulations and  
261 GLODAP data reported that in the Coral Sea, the present-day values of aragonite  
262 saturation state are much less than the 3.5 threshold (Guinotte et al., 2003). These  
263 differences are explained by their correction of the CMIP5 simulations to GLODAP  
264 DIC and TALK values (Key et al., 2004) that have very few measurements in this  
265 region.

266 The annual mean state of pH for the period 2000-2009 is shown in Figure 5. In  
267 contrast with aragonite saturation state there is an increasing latitudinal gradient from  
268 ~8.1 in Northern Australia to ~8.14 in Southern Australia. The reconstructed values  
269 show good agreement with observations collected on the southern Papua New Guinea  
270 coast by Fabricius et al. (2011). However, south of Australia, the pH decreases again  
271 to values comparable with those seen in Northern Australia.

272 The spatial gradients of pH and aragonite saturation state as function of latitude are  
273 consistent with the large-scale gradients calculated from observations of carbonate  
274 chemistry from GLODAP (Key et al., 2004). The distribution of aragonite saturation  
275 state is set by both the large-scale distribution of SST, which shows a strong  
276 latitudinal gradient, and TALK. Consequently the spatial differences between  
277 aragonite saturation state and pH are driven by temperature e.g. Zeebe and Wolf-  
278 Galdrow (2001).

279

### 280 **4.3 The Seasonal Cycle**

281 The seasonal standard deviation (2-sigma) of aragonite saturation state and pH reveal  
282 large spatial differences in the magnitude of the seasonal variability (Figure 5, lower  
283 panels). Large seasonality in aragonite saturation state is evident at > 0.4 units. This  
284 spatial pattern of this seasonality is quite heterogeneous, with the largest variability  
285 occurring along the East Coast of Australia, in the Tasman Sea, and off Southern  
286 Australia. The low seasonal variability predicted in the Coral Sea means that  
287 aragonite saturation state is above 3.5 even in the winter months. Strong and  
288 heterogeneous seasonality in pH is also present at > 0.06 units, around Australia, with

289 the largest range in Southern Australia.

290 The locations of large seasonality in aragonite saturation state and pH off Southern  
291 Australia are associated with regions of deep winter mixing > 200m (Condie and  
292 Dunn, 2006). Here, the seasonal deepening of the mixed layer in winter supplies  
293 carbon, alkalinity and nutrients to the surface ocean, which in turn alter the chemistry  
294 of the surface waters inducing large seasonal variability in ocean acidification values  
295 in the surface ocean. That the large seasonal variability in aragonite saturation state is  
296 not associated with large seasonal variability in pH along the East Coast of Australia  
297 and in the Tasman Sea, suggests that here the dominant driver of seasonality  
298 variability is SST rather than ocean dynamics.

299 An important consequence of the decoupling of the spatial patterns of pH and  
300 aragonite saturation state is that the biological responses to ocean acidification at the  
301 seasonal scale may also be decoupled as the susceptibility to pH and aragonite  
302 saturation varies between organisms. This has implications for understanding  
303 ecosystem responses to ocean acidification.

304 Areas of large seasonal variability are also present along parts off northern Australia  
305 and off Papua New Guinea. These are primarily driven by large seasonal changes in  
306 sea surface salinity driving changes in TALK and DIC which influences the pH and  
307 aragonite saturation state.

308

#### 309 **4.4 Comparison with Takahashi et al (2014)**

310 In this section the reconstructed annual mean and seasonality of pH and aragonite  
311 saturation state are compared with those that calculated nominally for 2005  
312 (Takahashi et al., 2014); hereafter-denoted T14 (Figure 6). The data of T14 are based  
313 on oceanic pCO<sub>2</sub> measurements and regional potential alkalinity versus salinity  
314 relationships, at a resolution of 4°x5°. Since T14 excludes Equatorial Pacific (north of  
315 8°S) data and coastal data, we can only compare our results T14 away from these  
316 regions.

317 The T14 spatial pattern of annual mean aragonite saturation state appears to be in

318 reasonable agreement with our reconstruction for most waters around Australia. An  
319 exception is off Northwestern Australia where the mean aragonite saturation state of  
320 T14 appears to be an under-estimate. Large differences in the seasonal changes also  
321 occur off the east coast of Australia and to the South of Australia. The magnitude of  
322 the seasonal variability (in T14) is lower than our reconstruction.

323 The pH values of T14 and our reconstruction both show the highest values in the  
324 subtropical waters, although T14 mean values are higher off eastern Australia and  
325 lower to the South of Australia. Overall there is quite poor agreement in both the  
326 magnitude and spatial pattern of pH variability for most regions.

327 That the spatial pattern of the seasonal cycle of aragonite saturation state is not  
328 reproduced along the East Coast of Australia and in the Tasman Sea, and the  
329 variability in Southern Australia is not seen in either pH nor aragonite saturation state,  
330 suggests that while the seasonal response of SST is captured in T14, the seasonal  
331 ocean dynamics are not well represented. Furthermore the magnitude of the seasonal  
332 cycle appeared to be underestimated in T14, this likely reflects the coarser resolution  
333 of T14 product than our reconstruction ( $4^{\circ}\times 5^{\circ}$  vs.  $1^{\circ}\times 1^{\circ}$ ) and the spatial interpolation  
334 required to generate T14.

335 As a result of this analysis we believe that in the Australian region our reconstruction  
336 offers an improved and higher resolution representation of the mean state and  
337 seasonality than T14. This comparison also underscores the need for such ongoing  
338 regional analyses, and the limitations of using large-scale global products such as T14  
339 to understand regional variability and change.

340

#### 341 **4.5 Historical Changes**

342 The historical change in ocean acidification since 1870 is represented in Figure 7 by  
343 the changes in the mean annual values of pH and aragonite saturation state between  
344 the period 1870-1889 and 1990-2009. The corresponding changes in sea surface  
345 temperature (HadiSST; Rayner et al., 2003) are shown over the same period in Figure  
346 8, indicate a small net warming of the waters around Australia. This warming has  
347 been relatively uniform with the exception of the northern edge of the Southern

348 Ocean, and Southeastern Australia which has been identified as a marine hotspot  
349 Hobday and Pecl (2013). Consequently the SST changes alone cannot explain the  
350 large ocean acidification changes, suggesting these are due to changes in ocean  
351 carbon uptake, rather than changes in SST. The changes with time in pH and  
352 saturation state at the IMOS-NRS sites are plotted in Figure 9.

353 We estimate that over the last 120 years there has been a (spatial) mean decrease in  
354 aragonite saturation state of 0.49. However as illustrated in Figure 9, these decreases  
355 are not constant with time and the change in aragonite saturation state is accelerating.  
356 There is also a strong latitudinal gradient in magnitude of the decrease, with larger  
357 changes occurring in Northern Australian waters (Ningaloo and North Stradbroke  
358 Island) and smaller changes to the south (Maria Island). This pattern of change around  
359 Australia is consistent with large-scale chemical buffering capacity of the ocean  
360 (Revelle factor) which increases from  $\sim 9$  at the equator to  $>11$  at bottom of the study  
361 region e.g. Sabine et al. (2004).

362 Consistent with aragonite saturation state over the last 120 years there has been a net  
363 decrease in pH of 0.09 units, very close to the estimated global decrease of 0.1 pH by  
364 Caldeira and Wickett (2003) over a similar period. Consistent with aragonite  
365 saturation a strong latitudinal gradient in pH is evident, but it is the inverse. The  
366 largest changes in pH have occurred in Southern Australia e.g. Maria Island (Figure  
367 9), with the smallest changes in Northern Australian waters (e.g. Yongala (Figure 9) is  
368 about 75% of the change experienced in the south). This spatial response of pH is  
369 primarily set by the gradient of ocean mean temperature that acts to increase pH in  
370 colder waters (Figure 8).

371

#### 372 **4.7 Robustness of the reconstruction**

373 The reconstructed time series of aragonite saturation state and pH are driven wholly  
374 by SST and atmospheric CO<sub>2</sub>, thereby neglecting any changes in salinity and/or  
375 biological production. Observationally, studies have suggested that in some regions  
376 around Australia changes in salinity over the last 50 years have occurred e.g. Durack  
377 and Wijffels (2010), while other regions have remained constant over the last 200  
378 years e.g. Calvo et al. (2007). If we assume, consistent with Durack et al. (2012), that

379 the changes are related to evaporation – precipitation (E-P) rather than local riverine  
380 input which can have large local inputs of DIC, TALK and potentially nutrients  
381 (Hieronymus and Walin, 2013), then any increase in salinity can be treated as  
382 freshwater input only. Consequently given the small trends, relative to the mean, and  
383 the very low sensitivity of oceanic  $p\text{CO}_2$  to freshwater input ( $< 1\%$ ), it is highly  
384 unlikely that such changes would make such a significant difference on pH or  
385 aragonite over the last 50 years. This is perhaps not surprising given that freshwater  
386 water changes act as a dilution flux i.e. acting equally on DIC and total alkalinity  
387 (Lenton et al., 2012).

388

389 The roles of nutrients driving variability and change in ocean acidification are also not  
390 considered in this study, as we assume that nutrients are zero around Australia. While  
391 this is not strictly true, most waters around Australia are oligotrophic in nature  
392 (Condie and Dunn, 2006). If the climatological values of silicate and nitrate from  
393 CARS (Ridgway et al., 2002) are used to calculate carbonate chemistry, we find only  
394 a small bias (0.0007 in aragonite saturation state and 0.005 in pH) in our  
395 reconstruction (well within the uncertainty). While we would like to have used a time-  
396 evolving field, analogous to salinity, at present no long-term time series are available  
397 to use in this reconstruction.

398 In this study we assumed that the seasonal air-sea disequilibrium ( $\Delta p\text{CO}_2$ ) is  
399 seasonally time invariant i.e. no interannual variability. While some studies have  
400 argued this variability maybe important at shorter-term timescales e.g. Sitch et al  
401 (2015), it is less clear how important these are on longer time series e.g. McKinley et  
402 al (2011). This is further complicated as the existing products of oceanic  $p\text{CO}_2$  fields  
403 e.g. Landschützer et al. (2014) only extend back in time several decades reflecting the  
404 limit of historical observations. Nevertheless to assess how important this term could  
405 be, we assumed an upper bound from the published study of McNeil and Matear  
406 (2008) who, in the more dynamically and biologically active Southern Ocean,  
407 calculated the error introduced by assuming a fixed (air-sea) disequilibrium term.  
408 From this study we can see that for an equivalent increase in (future) atmospheric  $\text{CO}_2$   
409 levels, that the error introduced into our calculation of pH and aragonite saturation  
410 state falls well within the reported uncertainty of our reconstruction.

411 **5. Conclusion**

412 To explore how Australia's marine environment has changed, we have synthesized  
413 newly acquired in-situ observations of carbon chemistry around Australia to: (i)  
414 provide an new estimate of the mean state and seasonality of pH and aragonite  
415 saturation state; and (ii) reconstruct the changes in ocean acidification around  
416 Australia since 1870.

417 In this work we developed a new total alkalinity-salinity relationship for the  
418 Australian region. This relationship was used in conjunction with observed salinity  
419 and oceanic and atmospheric CO<sub>2</sub> and SST data, to reconstruct the present and past  
420 changes in pH and aragonite saturation state. Our reconstructed fields were compared  
421 against the Takahashi et al (2014) climatology, and high-resolution data collected at  
422 the IMOS-NRS sites. We found good agreement between our reconstructed fields for  
423 the observed annual mean and seasonal cycles at the shelf IMOS-NRS sites except  
424 regions such as the Great Barrier Reef where near shore processes and coral reef  
425 metabolism could alter the pH and saturation state.

426 Our regional reconstruction provides much higher spatial and temporal resolution than  
427 previous global estimates. This highlights the importance of regional analyses and  
428 reconstructions in estimating and understanding region changes. An important result  
429 of this study is that at present the Coral Sea is not experiencing marginal conditions  
430 (values of aragonite saturation state < 3.5) with respect to ocean acidification as has  
431 been suggested.

432 Large changes in aragonite saturation state and pH have occurred over the last 140  
433 years in response to increasing oceanic uptake of atmospheric CO<sub>2</sub>. A net (spatial)  
434 mean decrease in pH of 0.09 is seen in the period (1990-2009) – (1889-1870),  
435 together with a net decrease in aragonite saturation state of 0.49, both of which are  
436 consistent with previous estimates of the historical changes. Importantly, due to ocean  
437 chemistry, the spatial pattern of the change in aragonite saturation state and pH are  
438 different. In this study we found the largest changes in aragonite saturation state  
439 occurred at mid and low latitudes, and the largest changes in pH occurred at higher  
440 latitudes.

441 The large seasonal variability around Australia is heterogeneous, with distinctly

442 different spatial patterns in aragonite saturation state and pH, with the exception of  
443 from South of Australia where variability is driven by deep winter mixing. For  
444 aragonite saturation state, large seasonal variability occurs off the East Coast of  
445 Australia and in Tasman Sea driven by seasonal variability in ocean temperatures  
446 That the variability in aragonite saturation state and pH are spatially different over  
447 temporal and regional scales, implies that biological responses and impacts are likely  
448 vary. Further, this suggests that both pH and aragonite (or calcite) saturation state  
449 need to be considered independently in assessing ecosystem responses and changes.  
450 This historical reconstruction also provides useful information to link with biological  
451 observations to help understand observed changes and aid in the design of future  
452 work, thereby elucidating the consequences of Ocean Acidification. To facilitate this  
453 all of the reconstructed data is available at <http://imos.aodn.org.au>

## 454 **6. Acknowledgments**

455 AL, BT and RJM acknowledge support from the Australian Climate Change Science  
456 Program. TPS would like to acknowledge funding support for the CSIRO carbon  
457 cluster. YN was supported by JSPS KAKENHI Grant Number 26220102. The  
458 authors would like to thank the Integrated Marine Observing System (IMOS) for  
459 providing data from the Australian National Research Sites (NRSs), and Kate Berry  
460 and Kristina Patterson for their analysis of the observed carbon data.

461 **7. References**

- 462 Albright, R., Langdon, C., and Anthony, K. R. N.: Dynamics of seawater carbonate  
463 chemistry, production, and calcification of a coral reef flat, Central Great Barrier Reef,  
464 *Biogeosciences*, 10, 6747-6758, 2013.
- 465 Antonov, J. I., Seidov, D., Boyer, T. P., Locarnini, R. A., Mishonov, A. V., Garcia, H. E.,  
466 Baranova, O. K., Zweng, M. M., and Johnson, D. R., *World Ocean Atlas 2009, Volume 2:*  
467 *Salinity*, in, edited by: Levitus, S., NOAA Atlas NESDIS 69, U.S. Government Printing  
468 Office, Washington, D.C., 184 pp, 2010
- 469 Bell, J. D., JE, J., and AJ, H.: Vulnerability of Tropical Pacific Fisheries and Aquaculture to  
470 Climate Change, Secretariat of the Pacific Community, Noumea, New Caledonia, 2011.
- 471 Caldeira, K., and Wickett, M. E.: Anthropogenic carbon and ocean pH, *Nature*, 425, 365-365,  
472 Doi 10.1038/425365a, 2003.
- 473 Calvo, E., Marshall, J. F., Pelejero, C., McCulloch, M. T., Gagan, M. K., and Lough, J. M.:  
474 Interdecadal climate variability in the Coral Sea since 1708 AD, *Palaeogeogr Palaeocl*, 248,  
475 190-201, Doi 10.1016/J.Palaeo.2006.12.003, 2007.
- 476 Ciais, P., Sabine, C., Bala, G., Bopp, L., Brovkin, V., Canadell, J., Chhabra, A., Defriers, R.,  
477 Galloway, J. N., Heinman, M., Jones, C. D., Le Quéré, C., Myneni, R. B., Piao, S., and  
478 Thornton, P.: Carbon and Other Biogeochemical Cycles, in: *Climate Change 2013: The*  
479 *Physical Science Basis. Contribution of Working Group I to the Fifth Assessment Report of*  
480 *the Intergovernmental Panel on Climate Change* edited by: Stocker, T. F., Qin, D., Plattner,  
481 G.-K., Tignor, M., Allen, S. K., Boschung, A., A, N., Xia, Y., V., B., and Midgley, P. M.,  
482 Cambridge University Press, Cambridge, United Kingdom and New York 2013.
- 483 Condie, S. A., and Dunn, J. R.: Seasonal characteristics of the surface mixed layer in the  
484 Australasian region: implications for primary production regimes and biogeography, *Marine*  
485 *and Freshwater Research*, 57, 569-590, Doi 10.1071/Mf06009\_Lr, 2006.
- 486 Dickson, A. G., and F. J. Millero, A comparison of the equilibrium constants for the  
487 dissociation of carbonic acid in seawater media, *Deep Sea Res., Part I*, 34, 1733-1743,  
488 doi:10.1016/0198-0149(87)90021-5, 1987
- 489 Doney, S. C., Balch, W. M., Fabry, V. J., and Feely, R. A.: Ocean Acidification: A Critical  
490 Emerging Problem for the Ocean Sciences, *Oceanography*, 22, 16-+, Doi  
491 10.5670/Oceanog.2009.93, 2009.
- 492 Doney, S. C., Ruckelshaus, M., Duffy, J. E., Barry, J. P., Chan, F., English, C. A., Galindo, H.  
493 M., Grebmeier, J. M., Hollowed, A. B., Knowlton, N., Polovina, J., Rabalais, N. N.,  
494 Sydeman, W. J., and Talley, L. D.: Climate Change Impacts on Marine Ecosystems, *Annu*  
495 *Rev Mar Sci*, 4, 11-37, Doi 10.1146/Annurev-Marine-041911-111611, 2012.



496 Dore, J. E., Lukas, R., Sadler, D. W., Church, M. J., and Karl, D. M.: Physical and  
497 biogeochemical modulation of ocean acidification in the central North Pacific, *P Natl Acad*  
498 *Sci USA*, 106, 12235-12240, Doi 10.1073/Pnas.0906044106, 2009.

499 Durack, P. J., and Wijffels, S. E.: Fifty-Year Trends in Global Ocean Salinities and Their  
500 Relationship to Broad-Scale Warming, *Journal of Climate*, 23, 4342-4362, Doi  
501 10.1175/2010jcli3377.1, 2010.

502 Durack, P. J., Wijffels, S. E., and Matear, R. J.: Ocean Salinities Reveal Strong Global Water  
503 Cycle Intensification During 1950 to 2000, *Science*, 336, 455-458, Doi  
504 10.1126/Science.1212222, 2012.

505 Fabricius, K. E., Langdon, C., Uthicke, S., Humphrey, C., Noonan, S., De'ath, G., Okazaki,  
506 R., Muehllehner, N., Glas, M. S., and Lough, J. M.: Losers and winners in coral reefs  
507 acclimatized to elevated carbon dioxide concentrations, *Nat Clim Change*, 1, 165-169, Doi  
508 10.1038/Nclimate1122, 2011.

509 Fabry, V. J., Seibel, B. A., Feely, R. A., and Orr, J. C.: Impacts of ocean acidification on  
510 marine fauna and ecosystem processes, *Ices J Mar Sci*, 65, 414-432, Doi  
511 10.1093/Icesjms/Fsn048, 2008.

512 Frolicher, T. L., and Joos, F.: Reversible and irreversible impacts of greenhouse gas emissions  
513 in multi-century projections with the NCAR global coupled carbon cycle-climate model, *Clim*  
514 *Dynam*, 35, 1439-1459, Doi 10.1007/S00382-009-0727-0, 2010.

515 Gagliano, M., McCormick, M. I., Moore, J. A., and Depczynski, M.: The basics of  
516 acidification: baseline variability of pH on Australian coral reefs, *Marine Biology*, 157, 1849-  
517 1856, Doi 10.1007/S00227-010-1456-Y, 2010.

518 Garcia, H. E., Locarnini, R. A., Boyer, T. P., Antonov, J. I., Baranova, O. K., Zweng, M. M.,  
519 and Johnson, D. R. (2010a), *World Ocean Atlas 2009, Volume 3: Dissolved Oxygen*  
520 *Apparent Oxygen Utilization, and Oxygen Saturation*, in, edited by: Levitus, S., NOAA Atlas  
521 NESDIS 70, U.S. Government Printing Office, Washington, D.C., 344 pp.

522 Garcia, H. E., Locarnini, R. A., Boyer, T. P., Antonov, J. I., Zweng, M. M., Baranova, O. K.,  
523 and Johnson, D. R., *World Ocean Atlas 2009, Volume 4: Nutrients (phosphate, nitrate,*  
524 *silicate)*, in, edited by: Levitus, S., NOAA Atlas NESDIS 71, U.S. Government Printing  
525 Office, Washington, D.C., 398 pp., 2010b

526 Garcia, H. E., Locarnini, R. A., Boyer, T. P., Antonov, J. I., Baranova, O. K., Zweng, M. M.,  
527 Reagan, J. R., and Johnson, D. R., *World Ocean Atlas 2013, Volume 3: Dissolved Oxygen,*  
528 *Apparent Oxygen Utilization, and Oxygen Saturation*, in, edited by: Levitus, S., and  
529 Mishonov, A., NOAA Atlas NESDIS 75, 27 pp, 2014a

530

531 Garcia, H. E., Locarnini, R. A., Boyer, T. P., Antonov, J. I., Baranova, O. K., Zweng, M. M.,  
532 Reagan, J. R., and Johnson, D. R., World Ocean Atlas 2013, Volume 4: Dissolved Inorganic  
533 Nutrients (phosphate, nitrate, silicate), in, edited by: Levitus, S., and Mishonov, A., NOAA  
534 Atlas NESDIS 76, 25, 25 pp., 2014b

535 Guinotte, J. M., Buddemeier, R. W., and Kleypas, J. A.: Future coral reef habitat marginality:  
536 temporal and spatial effects of climate change in the Pacific basin, *Coral Reefs*, 22, 551-558,  
537 Doi 10.1007/S00338-003-0331-4, 2003.

538 Hauck, J., and C. Völker, Rising atmospheric CO<sub>2</sub> leads to large impact of biology on  
539 Southern Ocean CO<sub>2</sub> uptake via changes of the Revelle factor, *Geophys. Res. Lett.*, 42,  
540 1459–1464, doi:10.1002/2015GL063070, 2015

541 Hieronymus, J., and Walin, G.: Unravelling the land source: an investigation of the processes  
542 contributing to the oceanic input of DIC and alkalinity, *Tellus B*, 65, Artn 19683 Doi  
543 10.3402/Tellusb.V65i0.19683, 2013.

544 Hobday, A. J., and Pecl, G. T.: Identification of global marine hotspots: sentinels for change  
545 and vanguards for adaptation action, *Rev Fish Biol Fisheries*, 10.1007/s11160-013-9326-6,  
546 2013.

547 Iglesias-Rodriguez, M. D., Halloran, P. R., Rickaby, R. E. M., Hall, I. R., Colmenero-  
548 Hidalgo, E., Gittins, J. R., Green, D. R. H., Tyrrell, T., Gibbs, S. J., von Dassow, P., Rehm,  
549 E., Armbrust, E. V., and Boessenkool, K. P.: Phytoplankton calcification in a high-CO<sub>2</sub>  
550 world, *Science*, 320, 336-340, Doi 10.1126/Science.1154122, 2008.

551 Key, R. M., Kozyr, A., Sabine, C. L., Lee, K., Wanninkhof, R., Bullister, J. L., Feely, R. A.,  
552 Millero, F. J., Mordy, C., and Peng, T. H.: A global ocean carbon climatology: Results from  
553 Global Data Analysis Project (GLODAP), *Global Biogeochemical Cycles*, 18, Artn Gb4031  
554 Doi 10.1029/2004gb002247, 2004.

555 Kuchinke, M., Tilbrook, B., and Lenton, A.: Seasonal variability of aragonite saturation state  
556 in the Western Pacific, *Mar Chem*, 161, 1-13, Doi 10.1016/J.Marchem.2014.01.001, 2014.

557 Langdon, C.: Effect of elevated pCO<sub>2</sub> on photosynthesis and calcification of corals and  
558 interactions with seasonal change in temperature/irradiance and nutrient enrichment, *Journal*  
559 *of Geophysical Research*, 110, 10.1029/2004jc002576, 2005.

560 Le Quéré, C., Moriarty, R., Andrew, R. M., Peters, G. P., Ciais, P., Friedlingstein, P., Jones,  
561 S. D., Sitch, S., Tans, P., Arneeth, A., Boden, T. A., Bopp, L., Bozec, Y., Canadell, J. G.,  
562 Chini, L. P., Chevallier, F., Cosca, C. E., Harris, I., Hoppema, M., Houghton, R. A., House, J.  
563 I., Jain, A. K., Johannessen, T., Kato, E., Keeling, R. F., Kitidis, V., Klein Goldewijk, K.,  
564 Koven, C., Landa, C. S., Landschützer, P., Lenton, A., Lima, I. D., Marland, G., Mathis, J. T.,  
565 Metzl, N., Nojiri, Y., Olsen, A., Ono, T., Peng, S., Peters, W., Pfeil, B., Poulter, B., Raupach,  
566 M. R., Regnier, P., Rödenbeck, C., Saito, S., Salisbury, J. E., Schuster, U., Schwinger, J.,

567 S  ferian, R., Segschneider, J., Steinhoff, T., Stocker, B. D., Sutton, A. J., Takahashi, T.,  
568 Tilbrook, B., van der Werf, G. R., Viovy, N., Wang, Y. P., Wanninkhof, R., Wiltshire, A.,  
569 and Zeng, N.: Global carbon budget 2014, 7, 47-85, doi:10.5194/essd-7-47-2015, 2015.

570 Lee, K., Tong, L. T., Millero, F. J., Sabine, C. L., Dickson, A. G., Goyet, C., Park, G. H.,  
571 Wanninkhof, R., Feely, R. A., and Key, R. M.: Global relationships of total alkalinity with  
572 salinity and temperature in surface waters of the world's oceans, *Geophys Res Lett*, 33, -, Artn  
573 L19605 Doi 10.1029/2006gl027207, 2006.

574 Lenton, A., Metzl, N., Takahashi, T., Kuchinke, M., Matear, R. J., Roy, T., Sutherland, S. C.,  
575 Sweeney, C., and Tilbrook, B.: The observed evolution of oceanic pCO<sub>2</sub> and its drivers over  
576 the last two decades, *Global Biogeochemical Cycles*, 26, Artn Gb2021, Doi  
577 10.1029/2011gb004095, 2012.

578 Lima, F. P., and Wethey, D. S.: Three decades of high-resolution coastal sea surface  
579 temperatures reveal more than warming, *Nat Commun*, 3, Artn 704  
580 Doi 10.1038/Ncomms1713, 2012.

581 Locarnini, R. A., Mishonov, A. V., Antonov, J. I., Boyer, T. P., Garcia, H. E., Baranova, O.  
582 K., Zweng, M. M., and Johnson, D. R., *World Ocean Atlas 2009, Volume 1: Temperature*, in,  
583 edited by: Levitus, S., Ed. NOAA Atlas NESDIS 68, U.S. Government Printing Office,  
584 Washington, D.C., 184 pp., 2010

585 Locarnini, R. A., Mishonov, A. V., Antonov, J. I., Boyer, T. P., Garcia, H. E., Baranova, O.  
586 K., Zweng, M. M., Paver, C. R., Reagan, J. R., Johnson, D. R., Hamilton, M., and Seidov, D.  
587 *World Ocean Atlas 2013, Volume 1: Temperature*, in, edited by: S. Levitus, E., and A.  
588 Mishonov, T. E., NOAA Atlas NESDIS 73, 40 pp, 2013

589 Lynch, T. P., Morello, E. B., Evans, K., Richardson, A., Rochester, J. W. C., Steinberg, C. R.,  
590 Roughan, M., Thompson, P., Middleton, J. F., Feng, M., Sherrington, R., Brando, V.,  
591 Tilbrook, B., Ridgway, K., Allen, S., Doherty, P., Hill, K., and Moltmann, T. C.: IMOS  
592 National Reference Stations: a continental wide physical, chemical and biological coastal  
593 observing system. , *PLOS One*, 9(12): e113652, doi:10.1371/journal.pone.0113652, 2014.

594 Matear, R. J., and Lenton, A.: Quantifying the impact of ocean acidification on our future  
595 climate, *Biogeosciences*, 11, 3965-3983, doi: 10.5194/Bg-11-3965-2014, 2014.

596 McNeil, B. I. and R.J. Matear: Southern Ocean acidification: A tipping point at 450-ppm  
597 atmospheric CO<sub>2</sub>, *PNAS* 105 (48), 18860-18864, doi: 10.1073/pnas.0806318105, 2008

598 McKinley, G. A., Fay, A. R., Takahashi, T., and N.Metzl: Convergence of atmospheric and  
599 North Atlantic carbon dioxide trends on multidecadal timescales, *Nature Geoscience*  
600 4, 606–610 doi:10.1038/ngeo1193, 2011

601 Mehrbach, C., C. H. Culberson, J. E. Hawley, and R. M. Pytkowicz, Measurement of the  
602 apparent dissociation constants of carbonic acid in seawater at atmospheric pressure, *Limnol.*

603 Oceanogr., 18, 897–907,doi:10.4319/lo.1973.18.6.0897, 1973.

604 Mucci, A.: The Solubility of Calcite and Aragonite in Seawater at Various Salinities,  
605 Temperatures, and One Atmosphere Total Pressure, Am J Sci, 283, 780-799, 1983.

606 Munday, P. L., Donelson, J. M., Dixson, D. L., and Endo, G. G. K.: Effects of ocean  
607 acidification on the early life history of a tropical marine fish, P Roy Soc B-Biol Sci, 276,  
608 3275-3283, Doi 10.1098/Rspb.2009.0784, 2009.

609 Munday, P. L., Dixson, D. L., McCormick, M. I., Meekan, M., Ferrari, M. C. O., and Chivers,  
610 D. P.: Replenishment of fish populations is threatened by ocean acidification, P Natl Acad Sci  
611 USA, 107, 12930-12934, doi:10.1073/Pnas.1004519107, 2010.

612 Pelejero, C., Calvo, E., McCulloch, M. T., Marshall, J. F., Gagan, M. K., Lough, J. M., and  
613 Opdyke, B. N.: Preindustrial to modern interdecadal variability in coral reef pH, Science, 309,  
614 2204-2207, Doi 10.1126/Science.1113692, 2005.

615 Rayner, N. A., Parker, D. E., Horton, E. B., Folland, C. K., Alexander, L. V., Rowell, D. P.,  
616 Kent, E. C., and Kaplan, A.: Global analyses of sea surface temperature, sea ice, and night  
617 marine air temperature since the late nineteenth century, J Geophys Res-Atmos, 108, Artn  
618 4407,doi:10.1029/2002jd002670, 2003.

619 Reynolds, R. W., Smith, T. M., Liu, C., Chelton, D. B., Casey, K. S., and Schlax, M. G.:  
620 Daily high-resolution-blended analyses for sea surface temperature, Journal of Climate, 20,  
621 5473-5496, Doi 10.1175/2007jcli1824.1, 2007.

622 Ricke, K. L., Orr, J. C., Schneider, K., and Caldeira, K.: Risks to coral reefs from ocean  
623 carbonate chemistry changes in recent earth system model projections, Environ Res Lett, 8,  
624 Artn 034003, Doi 10.1088/1748-9326/8/3/034003, 2013.

625 Ridgway, K. R., Dunn, J. R., and Wilkin, J. L.: Ocean interpolation by four-dimensional  
626 weighted least squares - application to the waters around Australasia, Journal of Atmospheric  
627 and Oceanic Technology, 19, 1357-1375, Doi 10.1175/1520-0426, 2002.

628 Riebesell, U., Fabry, V. J., Hansson, L., and Gattuso, J.-P.: Guide to best practices for ocean  
629 acidification research and data reporting, Publications Office of the European Union.,  
630 Luxembourg, 260, 2010.

631 Sabine, C. L., Feely, R. A., Gruber, N., Key, R. M., Lee, K., Bullister, J. L., Wanninkhof, R.,  
632 Wong, C. S., Wallace, D. W. R., Tilbrook, B., Millero, F. J., Peng, T. H., Kozyr, A., Ono, T.,  
633 and Rios, A. F.: The oceanic sink for anthropogenic CO<sub>2</sub>, Science, 305, 367-371, Doi  
634 10.1126/Science.1097403, 2004.

635 Sasse, T. P., McNeil, B. I., and Abramowitz, G.: A new constraint on global air-sea CO<sub>2</sub>  
636 fluxes using bottle carbon data, Geophys Res Lett, 40, 1594-1599, Doi 10.1002/Grl.50342,  
637 2013.

638 Shaw, E. C., McNeil, B. I., and Tilbrook, B.: Impacts of ocean acidification in naturally  
639 variable coral reef flat ecosystems, *J Geophys Res-Oceans*, 117, Artn C03038, Doi  
640 10.1029/2011jc007655, 2012.

641 Silverman, J., Lazar, B., Cao, L., Caldeira, K., and Erez, J.: Coral reefs may start dissolving  
642 when atmospheric CO<sub>2</sub> doubles, *Geophys Res Lett*, 36, Artn L05606  
643 Doi 10.1029/2008gl036282, 2009.

644 Stanley, S. M., and Hardie, L. A.: Secular oscillations in the carbonate mineralogy of reef-  
645 building and sediment-producing organisms driven by tectonically forced shifts in seawater  
646 chemistry, *Palaeogeogr Palaeoclimatol*, 144, 3-19, Doi 10.1016/S0031-0182(98)00109-6, 1998.

647 Takahashi, T., Sutherland, S. C., Wanninkhof, R., Sweeney, C., Feely, R. A., Chipman, D.  
648 W., Hales, B., Friederich, G., Chavez, F., Sabine, C., Watson, A., Bakker, D. C. E., Schuster,  
649 U., Metzl, N., Yoshikawa-Inoue, H., Ishii, M., Midorikawa, T., Nojiri, Y., Kortzinger, A.,  
650 Steinhoff, T., Hoppema, M., Olafsson, J., Arnarson, T. S., Tilbrook, B., Johannessen, T.,  
651 Olsen, A., Bellerby, R., Wong, C. S., Delille, B., Bates, N. R., and de Baar, H. J. W.:  
652 Climatological mean and decadal change in surface ocean pCO<sub>2</sub>, and net sea-air CO<sub>2</sub> flux  
653 over the global oceans, *Deep-Sea Res Pt II*, 56, 554-577, Doi 10.1016/J.Dsr2.2008.12.009,  
654 2009.

655 Sitch, S., Friedlingstein, P., Gruber, N., Jones, S. D., Murray-Tortarolo, G., Ahlström, A.,  
656 Doney, S. C., Graven, H., Heinze, C., Huntingford, C., Levis, S., Levy, P. E., Lomas, M.,  
657 Poulter, B., Viovy, N., Zaehle, S., Zeng, N., Arneth, A., Bonan, G., Bopp, L., Canadell, J. G.,  
658 Chevallier, F., Ciais, P., Ellis, R., Gloor, M., Peylin, P., Piao, S. L., Le Quéré, C., Smith, B.,  
659 Zhu, Z., and Myneni, R.: Recent trends and drivers of regional sources and sinks of carbon  
660 dioxide, *Biogeosciences*, 12, 653-679, doi:10.5194/bg-12-653-2015, 2015.

661 Takahashi, T., Sutherland, S. C., Chipman, D. W., Goddard, J. G., Ho, C., Newberger, T.,  
662 Sweeney, C., and Munro, D. R.: Climatological distributions of pH, pCO<sub>2</sub>, total CO<sub>2</sub>,  
663 alkalinity, and CaCO<sub>3</sub> saturation in the global surface ocean, and temporal changes at selected  
664 locations, *Mar Chem*, 164, 95-125, doi: 10.1016/j.marchem.2014.06.004, 2014.

665 Zeebe, R. E. and Wolf-Gladrow. CO<sub>2</sub> in Seawater: Equilibrium, Kinetics, Isotopes. Elsevier  
666 Oceanography Series, 65, pp. 346, Amsterdam, 2001

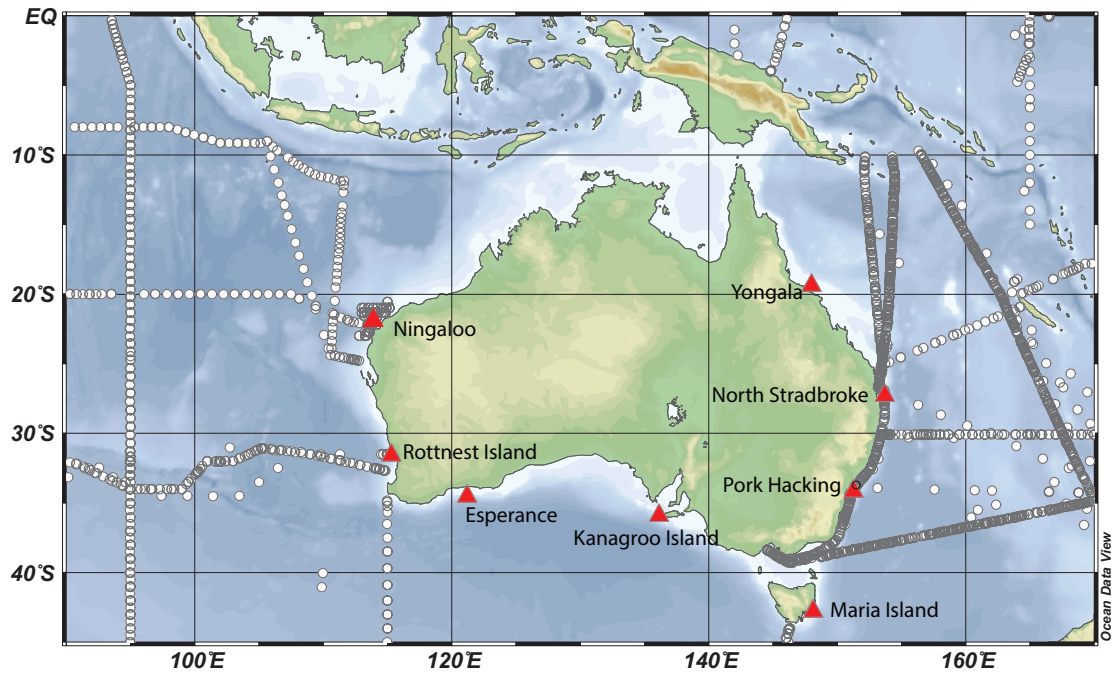
667 Zweng, M. M., Reagan, J. R., Antonov, J. I., Locarnini, R. A., Mishonov, A. V., Boyer, T. P.,  
668 Garcia, H. E., Baranova, O. K., Johnson, D. R., D. Seidov, and Biddle, M. M. (2013), World  
669 Ocean Atlas 2013, Volume 2: Salinity, in, edited by: Levitus, S., and Mishonov, A., NOAA  
670 Atlas NESDIS 74, 39 pp.

671

672

673

674 **7. Figures and Tables**



675

676

677 Figure 1 Locations (circles) of the concomitant measurements of alkalinity and  
678 salinity used to develop a new salinity-alkalinity relationship for the Australian  
679 Region, the cruises are listed in Table 1. Overlain on this plot (red triangles) are the  
680 locations of IMOS National Reference Stations (NRS) used in this study.

681

682

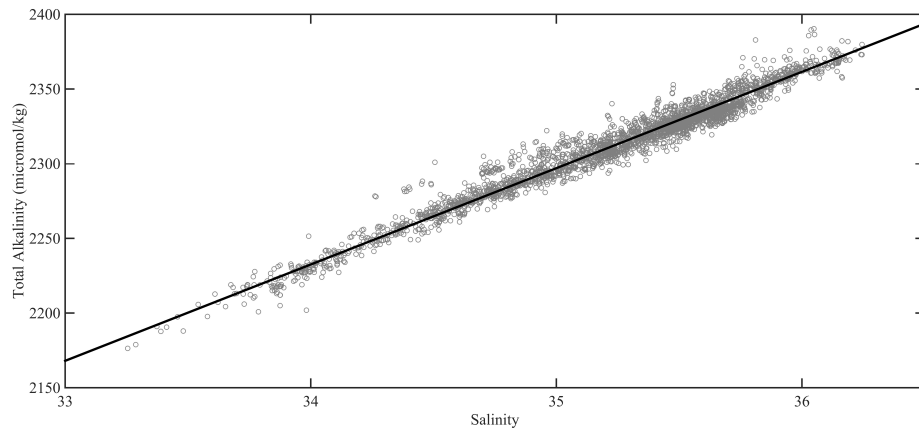
683

684

685

686

687



688

689

690 Figure 2 The new salinity-alkalinity relationship developed for the Australian Region

691 based on observations (Figure 1) collected in the period 1992-2011. The individual

692 cruises are listed in Table 1.

693

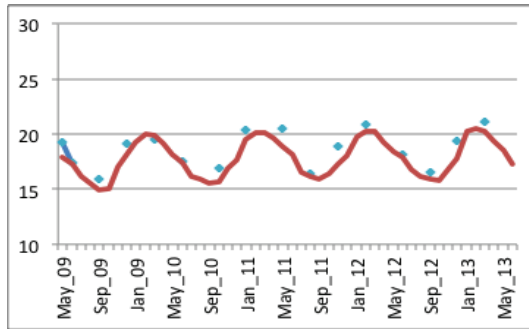
694

695

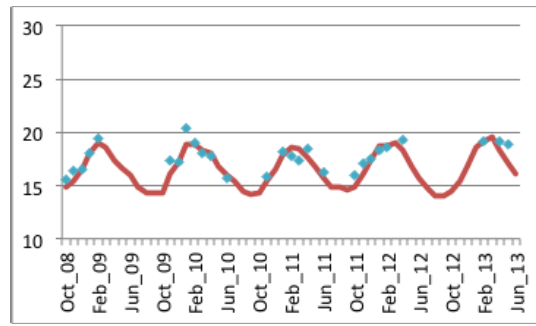
696

697

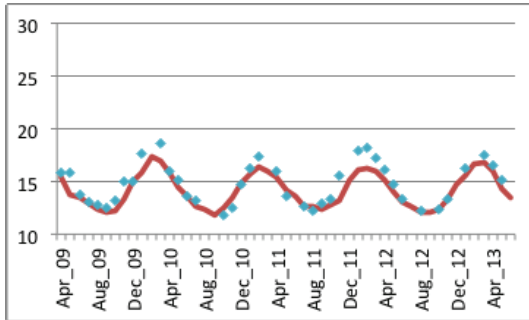
698



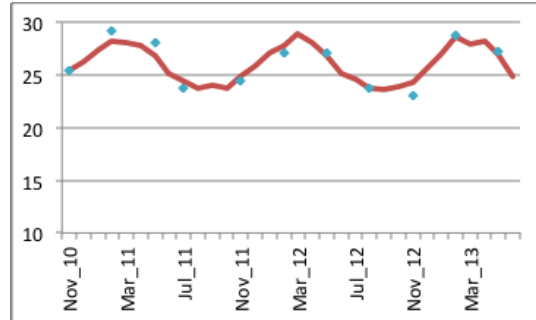
Esperance



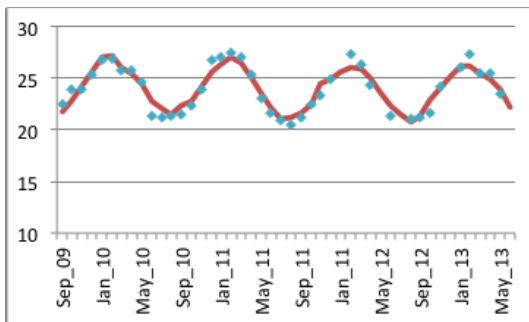
Kangaroo Island



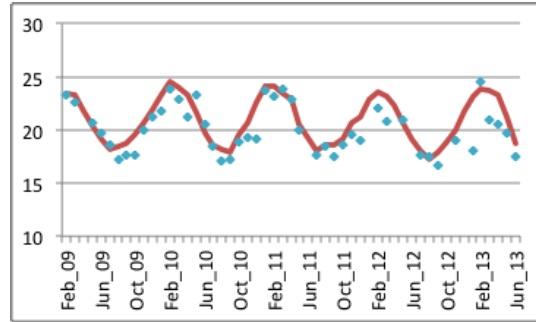
Maria Island



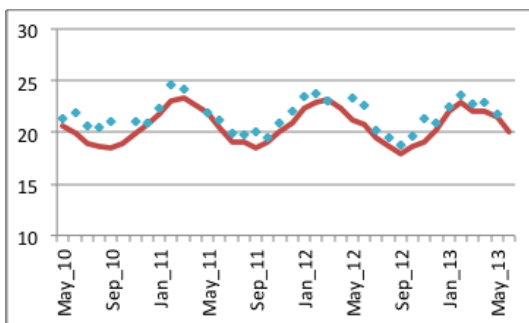
Ningaloo



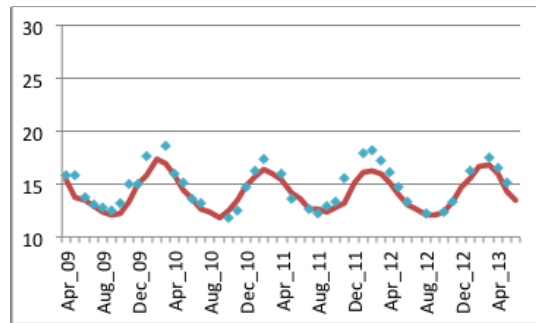
North Stradbroke



Port Hacking



Rottneest



Yongala

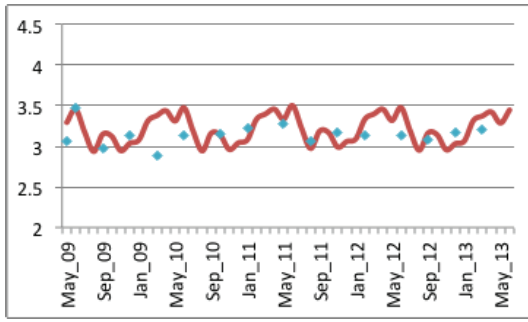
699

700

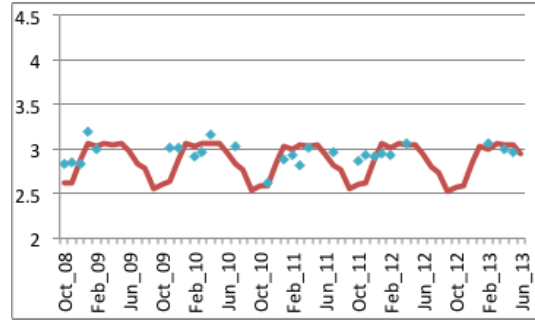
701

Figure 3 Comparison of sea surface temperature from the observations at the IMOS National Research Stations with HadiSST (Rayner et al, 2003)

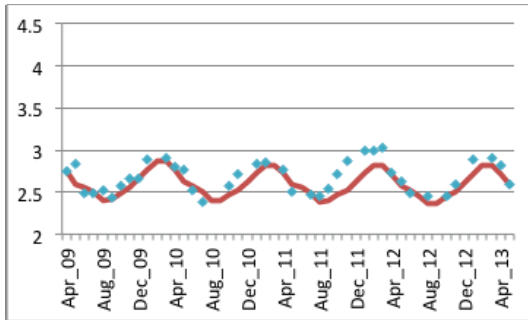




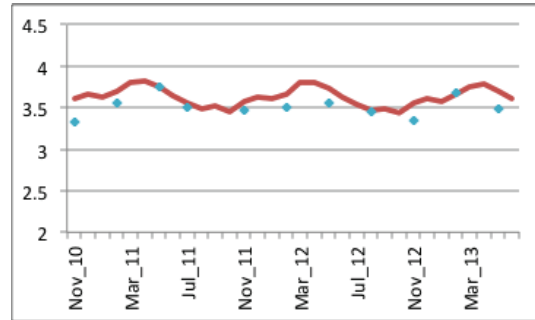
Esperance



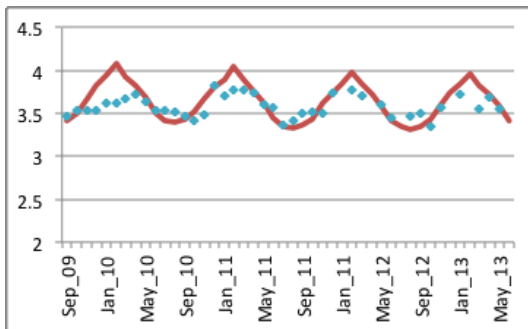
Kangaroo Island



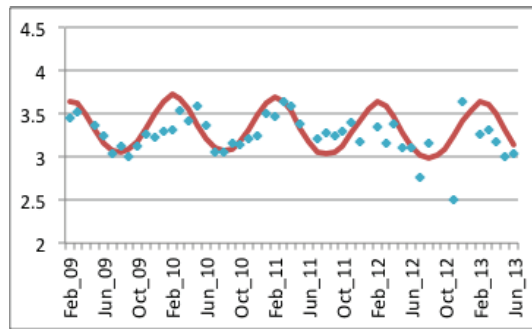
Maria Island



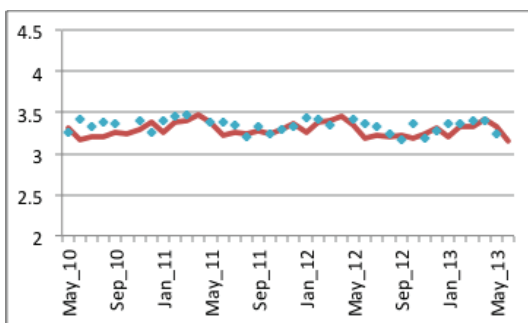
Ningaloo



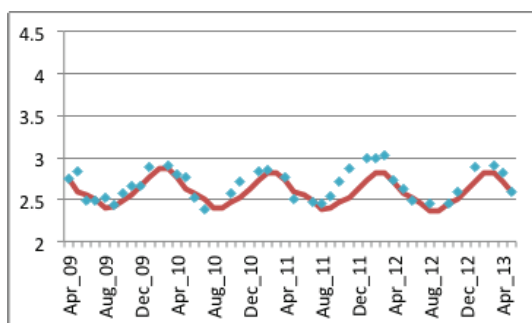
North Stradbroke



Port Hacking



Rottnest



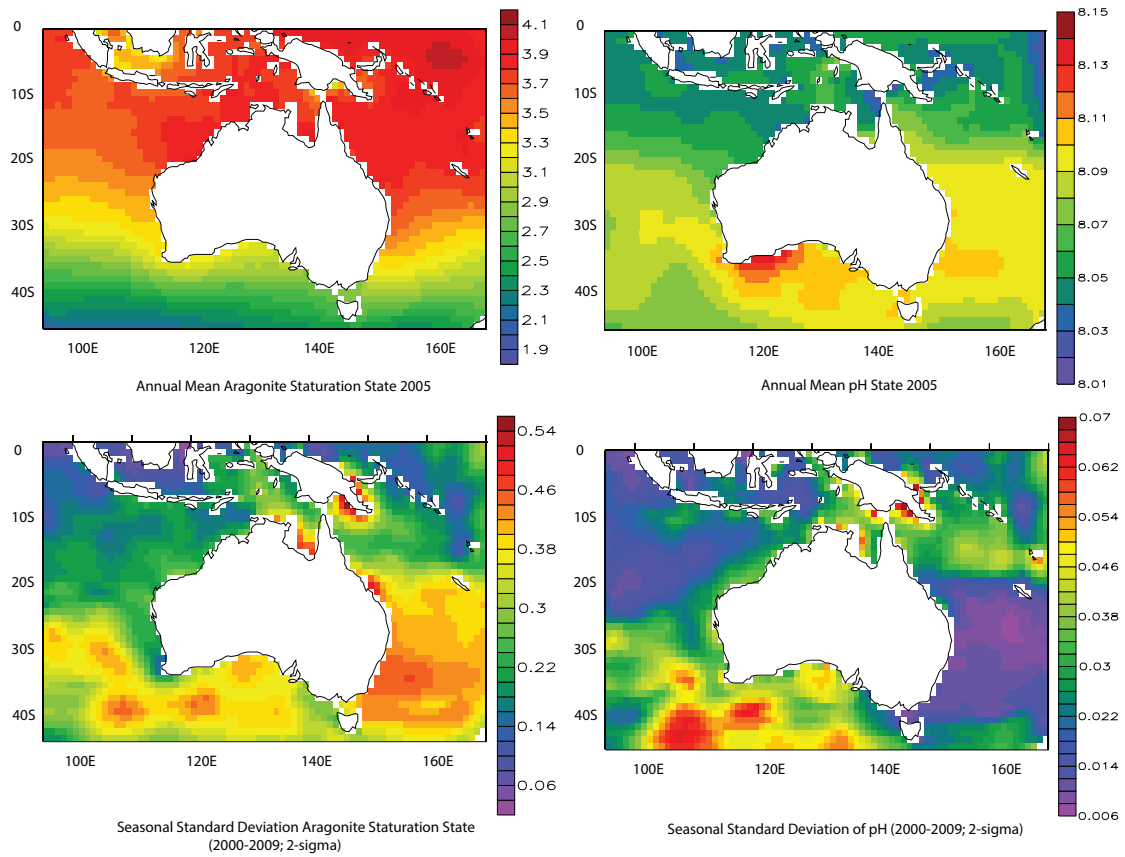
Yongala

702

703

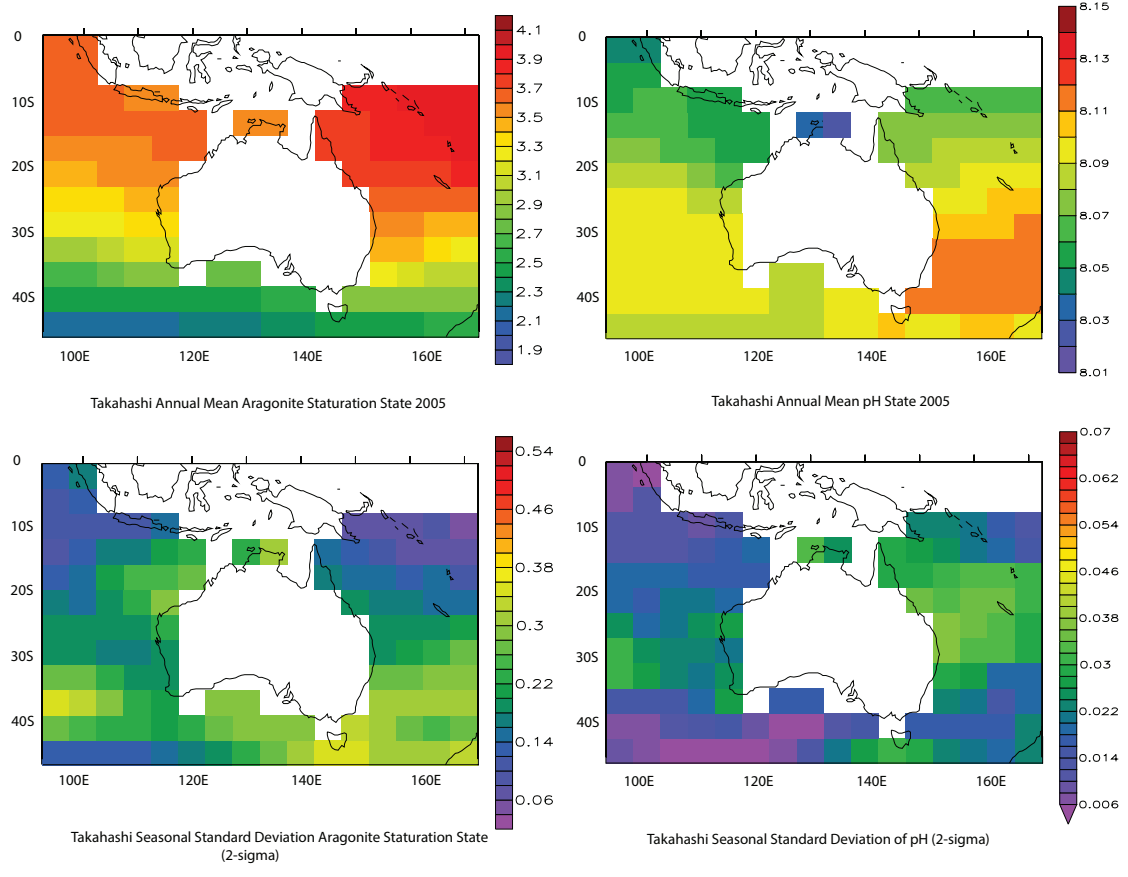
704 Figure 4 Comparison of aragonite saturation state ( $\Omega_{AR}$ ) from the observations at the

705 IMOS National Research Stations with the reconstructed values.



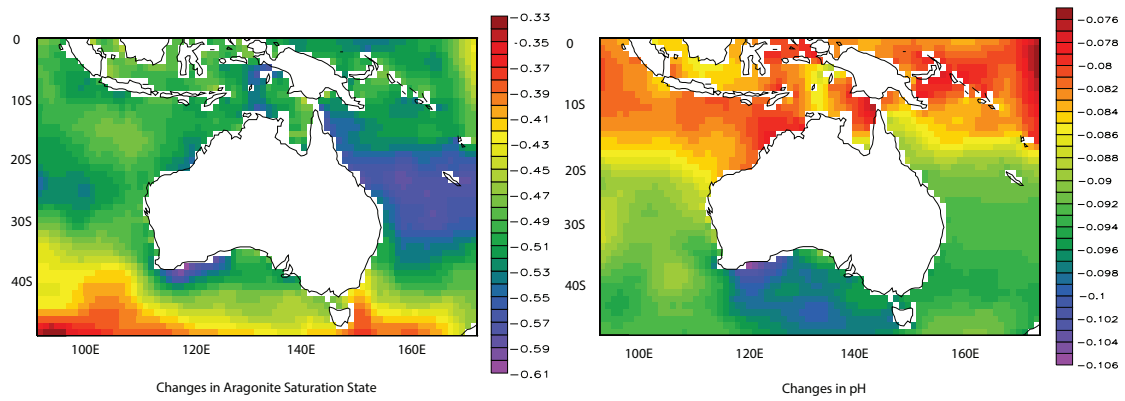
706  
 707  
 708  
 709  
 710  
 711  
 712  
 713

Figure 5 Upper: the reconstructed annual mean aragonite saturation state and pH for the period 2000-2009; Lower: the seasonal variability given by 2 times the standard deviation ( $2\text{-}\sigma$ ) of the seasonal variability in aragonite saturation state and pH from the period 2000-2009.



714  
 715  
 716  
 717  
 718  
 719  
 720  
 721  
 722  
 723  
 724  
 725

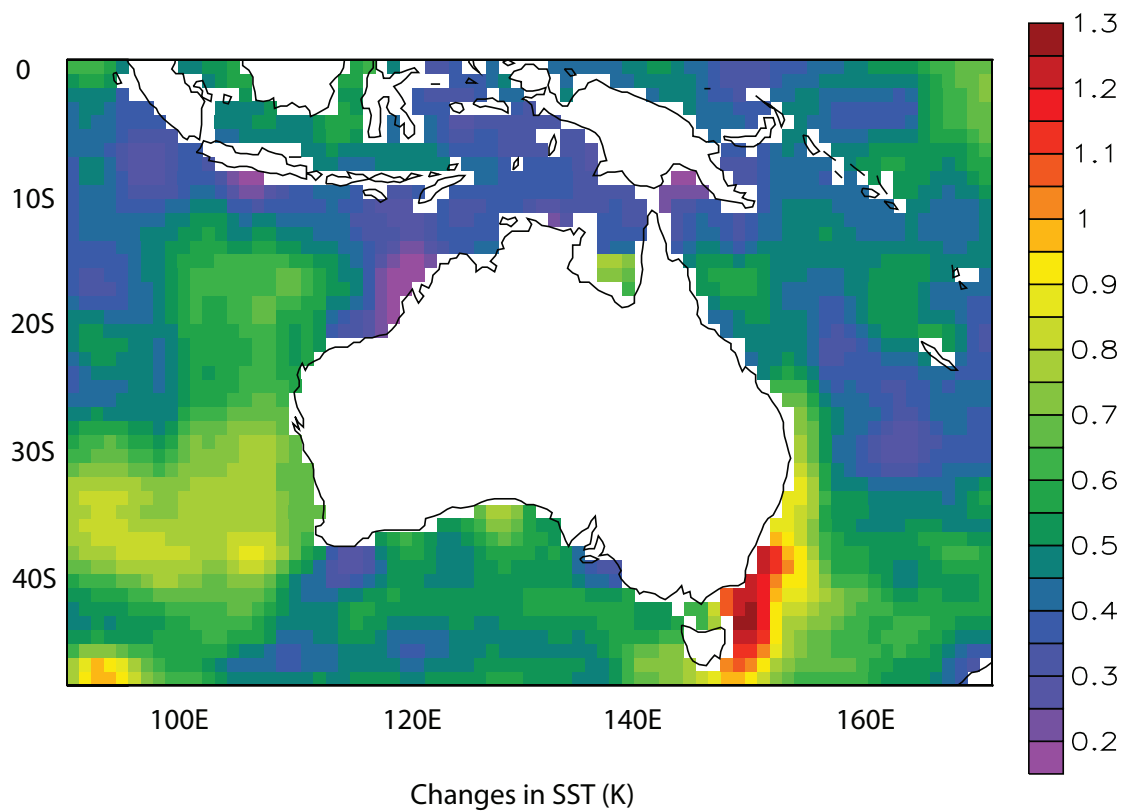
Figure 6 Upper: the annual mean aragonite saturation state and pH for 2005 from Takahashi et al (2014); Lower: standard deviation ( $2\sigma$ ) of the seasonal variability in aragonite saturation state and pH for 2005 from Takahashi et al (2014).



726

727

728 Figure 7 Annual mean 120-year differences (2000-2009 and 1880-1889) in aragonite  
 729 saturation state and pH.

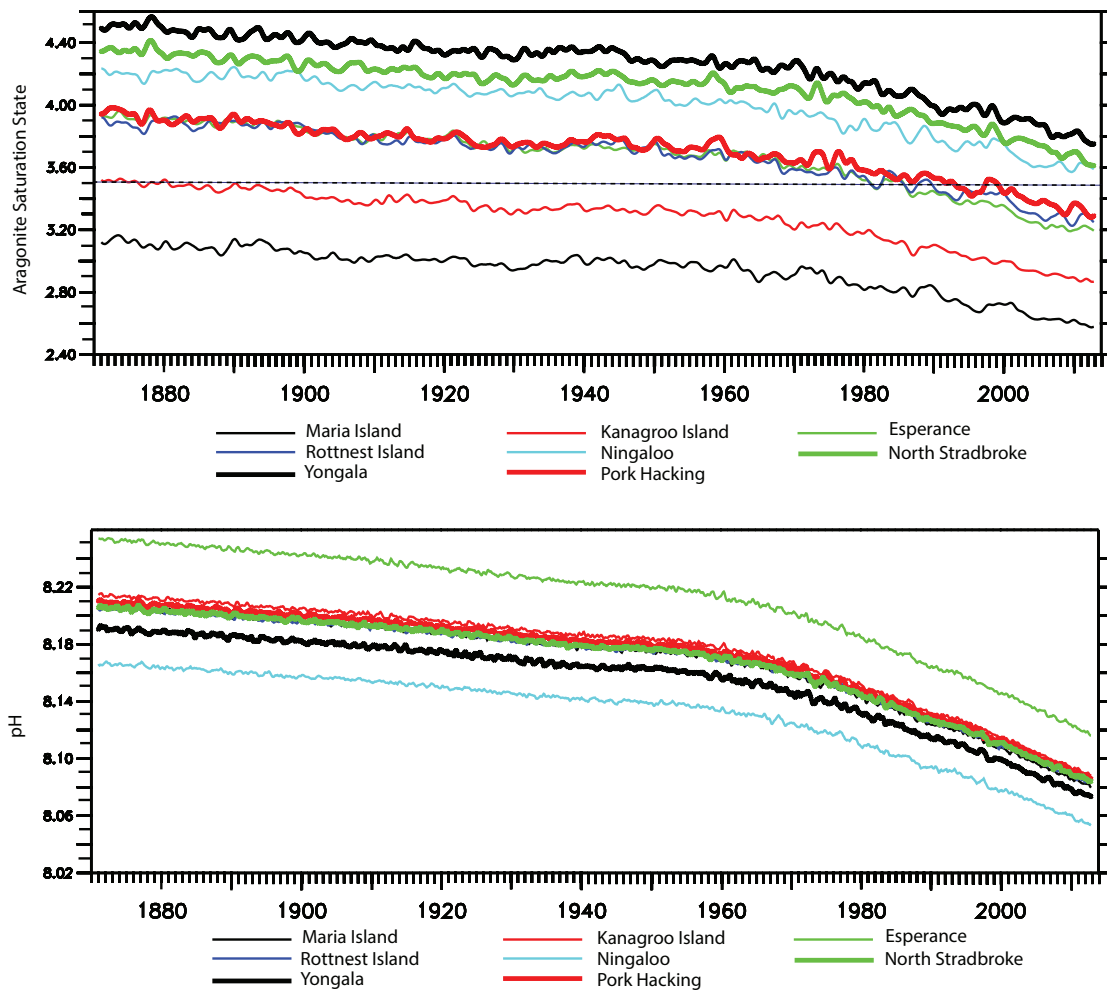


730

731

732 Figure 8 Annual mean 120-year differences (2000-2009 and 1880-1889) in SST.

733



734  
 735  
 736  
 737  
 738  
 739  
 740  
 741  
 742  
 743  
 744  
 745  
 746  
 747  
 748  
 749

Figure 9 Reconstructed time series of annual mean aragonite saturation state (upper) and pH (lower) at the IMOS-NRSs. Overlain on the upper plot is the threshold for the transition to marginal conditions for coral reefs (3.5) from Guinotte et al. (2003)

Voyage <sup>1</sup>	Region/ExPCODE	Latitude	Longitude	Period	Number
Section P13	West Pacific 31VIC92_0_1_2	0°S - 5°S	164°E - 165°E	Oct 1992	13
Section P10	West Pacific 3250TN026/1	0°S - 5°S	145°E - 146°E	Oct 1993	11
Section P21	Coral Sea 318M19940327	17°S - 25°S	155°E - 170°E	Jun 1994	49
Section P9	West Pacific 49RY9407_1	0°S - 3°S	142°E - 143°E	Aug 1994	7
FLUPAC	West Pacific 35A319940923	0°S - 15°S	165°E - 167°E	Sep 1994 - Oct 1994	66
Section I8S/I9S	Indian Ocean 316N145_5	32°S - 45°S	95°E - 115°E	Dec 1994 - Jan 1995	29
Section I9N	Indian Ocean 316N145_6	0°S - 32°S	93°E - 106°E	Jan 1995 - Feb 1995	100
Section SR3	Southern Ocean AR9404_1	44°S - 45°S	146°E - 147°E	Jan 1995 - Feb 1995	5
Section I8N/I5E	Indian Ocean 316N145_7	31°S - 34°S	91°E - 115°E	Apr 1995	57
Section I3	Indian Ocean 316N145_8	20°S - 22°S	90°E - 114°E	Apr 1995 - May 1995	31
Section	West Pacific 49HG19950414	1°S - 35°S	153°E - 163°E	Apr 1995 - May 1995	25
Section I4	Indian Ocean 3175MB95_07	31°S - 43°S	90°E - 110°E	Sep 1995 - Oct 1995	28
Section I10	Indian Ocean 316N145_13	9°S - 25°S	106°E - 112°E	Nov 1995	76
Section I2	Indian Ocean 316N145_14_15	8°S - 9°S	90°E - 106°E	Dec 1995	37
Section SR3	Southern Ocean 09AR19960822	44°S - 45°S	146°E - 147°E	Sep 1996 - Oct 1996	5
Section I2	Indian Ocean 09AR20000927	28°S - 34°S	94°E - 115°E	Sep 2000 - Nov 2000	66
Section SR3	Southern Ocean 09AR20011029	44°S - 45°S	146°E - 147°E	Oct 2001	7
Section I5	Indian Ocean 74AB20020301	31°S - 35°S	91°E - 115°E	Apr 2002	34
OISO-10	Southern Ocean 35MF20030123	45°S	146°E	Jan 2003	5
Section P6W	West Pacific 49NZ20030803	30°S	154°E - 170°E	Aug 2003	40
Section I3	Indian Ocean 49NZ20031209	20°S - 22°S	90°E - 113°E	Jan 2004	33
Section I9S	Southern Ocean I09S_09AR20041	35°S - 44°S	115°E	Dec 2004	18
Section P10	West Pacific 49NZ20050525	0°S - 4°S	145°E - 146°E	Jun 2005	18
TransFuture 5	Tasman Sea/ Coral Sea	10°S - 40°S	144°E - 172°E	Feb 2007 - Sep 2011	1460
Section I8S	Indian Ocean I08S_33RR20070	28°S - 45°S	94°E - 95°E	Mar 2007	79
Section I9N	Indian Ocean I09N_33RR20070	0°S - 28°S	93°E - 95°E	Mar 2007 - Apr 2007	103
Section I5	Indian Ocean I05_33RR200903	31°S - 35°S	90°E - 115°E	Apr 2009 - May 2009	128
Section P21	West Pacific 49NZ20090521	18°S - 25°S	154°E - 170°E	Jun 2009	52

Section P6W	West Pacific 318M20091121	30°S	154°E - 170°E	Nov 2009 - Dec 2009	93
SS201004	Indian Ocean	21°S - 23°S	112°E - 115°E	May 2010	92
Total					2772

750 <sup>1</sup> <http://cdiac.ornl.gov/ftp/oceans/>

751

752 Table 1. Cruise data used to derive the salinity versus total alkalinity relationship for

753 surface waters in Australian regional seas.

754

755

756

757

758

759

760

761

762

763

764

765

766

767

768

769

770

771

772

773

774

775

776

777

778

779

780

781  
 782  
 783  
 784

	Lat	Lon	SST - <i>BIAS</i>	SST - <i>R</i>	OmA - <i>BIAS</i>	OmA <i>-R</i>	n
Esperance	33° 56S	121° 51E	0.8	0.93	0.09	-0.06	16
Kangaroo Island	35° 49S	136° 27E	0.38	0.84	0.01	0.03	27
Maria Is	42° 36	148° 14E	0.6	0.93	0.07	0.83	40
Rottnest Is	32° 25S	115° 25S	1.01	0.92	0.06	0.26	33
Ningaloo	21° 52S	113° 57S	0.08	0.95	0.17	0.62	11
Yongala	19° 19S	147° 27S	0.13	0.94	0.27	0.45	37
Port Hacking	34° 5S	151° 6S	0.82	0.89	0.09	0.58	46
North Stradbroke	27° 18S	153° 6S	0.08	0.96	0.06	0.78	40

785  
 786  
 787  
 788  
 789  
 790  
 791  
 792  
 793  
 794  
 795  
 796  
 797

Table 2: The locations of the NRS sites used in this study, along with the biases, correlation coefficient (*R*) between the SST and aragonite saturation state observed at the site with values from our reconstruction, HadSST and calculated omega, respectively. Also listed are the number of observations used in calculating the Biases and Correlations